NJC

Accepted Manuscript

This is an *Accepted Manuscript*, which has been through the Royal Society of Chemistry peer review process and has been accepted for publication.

Accepted Manuscripts are published online shortly after acceptance, before technical editing, formatting and proof reading. Using this free service, authors can make their results available to the community, in citable form, before we publish the edited article. We will replace this *Accepted Manuscript* with the edited and formatted *Advance Article* as soon as it is available.

You can find more information about *Accepted Manuscripts* in the Information for Authors.

Please note that technical editing may introduce minor changes to the text and/or graphics, which may alter content. The journal's standard Terms & Conditions and the Ethical guidelines still apply. In no event shall the Royal Society of Chemistry be held responsible for any errors or omissions in this *Accepted Manuscript* or any consequences arising from the use of any information it contains.

ROYAL SOCIETY OF CHEMISTRY

www.rsc.org/njc

Graphical Abstract

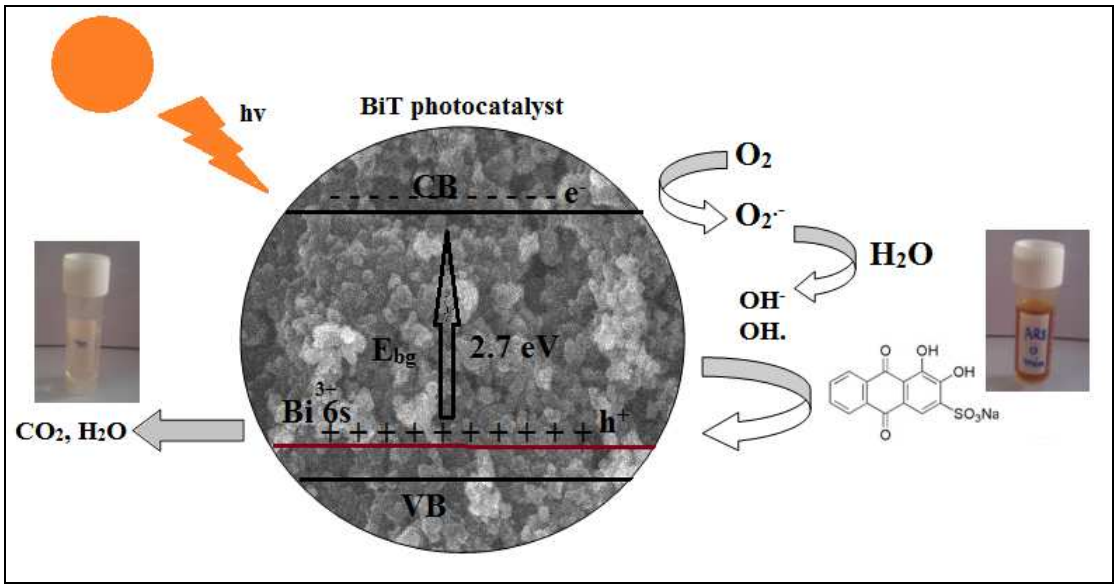

Visible-light-driven photocatalytic degradation of Alizarin red S using Bi-doped TiO_2 nanoparticles

Swati Sood[1], Surinder Kumar Mehta[1], Ahmad Umar[2,3]*, Sushil Kumar Kansal[4*]

[1]Department of Chemistry, Panjab University, Chandigarh-160014, India,
[2]Department of Chemistry, College of Science and Arts, Najran University, P.O.Box-1988, Najran-11001, Kingdom of Saudi Arabia,
[3]Promising Centre for Sensors and Electronic Devices (PCSED), Najran University, P.O.Box-1988, Najran-11001, Kingdom of Saudi Arabia
[4]Dr.S.S.B University Institute of Chemical Engineering & Technology, Panjab University, Chandigarh-160014, India

*Corresponding Authors:

Prof. Sushil Kumar Kansal : sushilkk1@yahoo.co.in; sushilkk1@pu.ac.in,

Prof. Ahmad Umar: ahmadumar786@gmail.com

Tel/Fax:+91-172-2534920, +966-534574597

Graphical Abstract

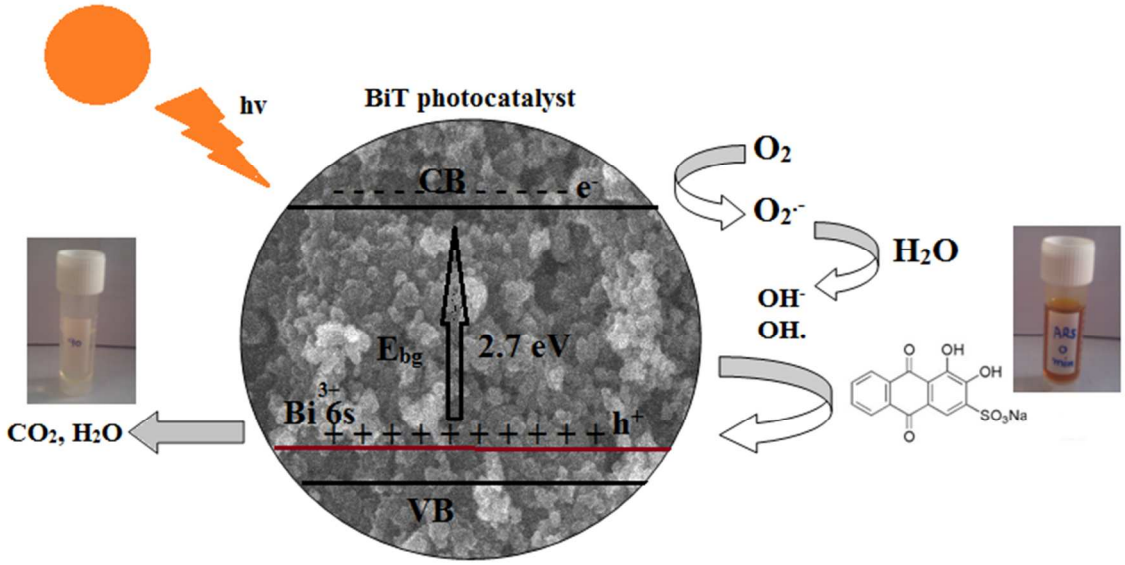

- Ultrasonic assisted sol-gel synthesized Bi doped TiO_2 nanoparticles
- Mesoporous nanoparticles having good crystallinity and high surface area
- 1% Bi doped TiO_2 catalyst showed highest photocatalytic activity under visible light

Abstract

In this paper we report the preparation of a series of Bi^{3+}-doped TiO_2 nanoparticles with different Bi-concentrations, i.e. 0.25%- 5%by a facile sol-gel process and their application as efficient photocatalyst. The detailed characterization revealed that the Bi doped TiO_2 catalysts possess densely grown nanoparticles, high specific surface area, crystalline anatase TiO_2 and good optical properties. The incorporation of Bi^{3+} into TiO_2 lattice lead to the expansion of TiO_2 spectral response into visible light and efficient separation of charge carriers. The prepared samples were employed for the photocatalytic degradation of Alizarin red S dye (ARS) under visible light illumination. It was found that the incorporation of Bi^{3+} ions in TiO_2lattice causes marked improvement in photocatalytic degradation of ARS dye; however, the degradation efficiency depended upon the Bi^{+3}ion doping concentration and dose of the prepared catalyst. The detailed photocatalytic experiments confirmed that the 1% Bi^{+3} ion doping concentration and 0.1 g/L dose exhibited best photocatalytic degradation efficiencies for the model dye. Moreover, more than 80% degradation of ARS was observed by the prepared Bi-doped catalysts within 90 minutes under visible-light. The synthesized Bi-doped TiO_2 nanoparticles revealed superior photocatalytic behavior towards the photocatalytic degradation of ARS under similar experimental conditions, as compared to the synthesized TiO_2 nanoparticles and other commercially available derivatives (TiO_2PC-50 and TiO_2 P25).

Keywords: Bi-doped TiO_2 nanoparticles; Alizarin red S; Visible-light-driven; Photocatalytic degradation

1. Introduction

A number of studies have been undertaken for efficient removal of hazardous organic molecules since past several decades.[1] Considering massive energy crisis and serious global environmental pollution issues, photocatalysis captures the centre stage as a green technology in harvesting solar energy and destroying organic contaminants.[1-7]TiO_2 presents itself as a leading photocatalyst owing to its numerous benefits e.g. easy availability, stability, non toxicity, chemical inertness and its efficacy in oxidation of versatile organic molecules.[8–14]However, its further practical application is restricted because of its wide energy band gap.$TiO_2$is photoactive only under the ultraviolet light (typically < 390 nm)rather than visible light which comprises almost 50% part of solar light.Moreover, overall quantum efficiency is further limited by electron–hole recombinations taking place at a faster rate.[13]To caterthese drawbacks, there have been numerous attempts by many researchers to tune the properties of $TiO_2$by coupling with other compounds[15-21]and doping with either anions[22–25] or cations[26–28],depending upon the type of precursors, solvents, molar ratio of the dopants and synthetic routes.

Doping is an efficientand easy strategy for overcoming the above said limitations and improving the catalytic behavior of TiO_2.In this regard; various visible light active catalysts have been prepared.[29-33]Especially, the catalysts doped with cations of d10 electronic configuration (eg. Bi^{3+}, In^{3+}, Al^{3+}or Ga^{3+})a re the most promising catalysts. Among these Bismuth compounded and doped photocatalysts grab a major attention. Bi^{3+} when incorporated into TiO_2 lattice, enhances the spectral range of $TiO_2$and inhibits electron-hole recombination, thus facilitating the photocatalysed reactions.[31-36]Lopez et al. successfully synthesized Bi doped TiO_2 catalysts by a sol–gel hydrothermal method. They proved that Bi^{3+} in TiO_2 catalystcauses marked increase in photocatalytic degradation efficiency for phenol in aqueous solution, depending upon the

optimum concentration of the Bi^{3+} and calcination treatments.[31]Xu and coworkers fabricated Bi-doped TiO_2nanofibres with varied Bi content by using an electro-spinning route[32]. Hu et al. synthesized Bi-doped TiO_2photocatalyst by simple mixing method. They found that the excess Bi_2O_3 loading (>5 mol%) and sol–gel transformations lead to the formation of Bi_xTiO_y[33]. Recently, TiO_2nanoparticles co-doped with Bi and N have been synthesized by hydrothermal and impregnation hydrolysis route and it was established that Bi species plays a crucial role in improvement of optical properties of the N–TiO_2 system[34]. Till now, considerable research has been dedicated to develop efficient Bi incorporated TiO_2 photocatalyst[31-39].However, more efforts arerequired to process efficient Bi-doped TiO_2photocatalyst with excellent stability, separation and photo-activity.

In this paper, we report a convenient ultrasonic assisted sol-gel route to synthesize Bi-doped TiO_2 with different Bi/Ti molar ratio, which have been further, characterized and investigated for the photocatalytic degradation of an anthraquinone dye, Alizarin red S (ARS). ARS finds wide applications in textile industry and is a serious environmental contaminant, so effective treatment methods need to be implied for the degradation of ARS dye in wastewater[2]. We hereby propose that this work will be significant for scientific as well as for practical application in the treatment of environmental pollution caused by widespread disposal of organic pollutants.

2. Experimental

2.1. Materials

All the chemicals used were of analytical grade. Titanium tetra-isopropoxide (TTiP) and bismuth (III) nitrate pentahydrate ($Bi(NO_3)_3.5H_2O$) were obtained from Aldrich (USA)and

Himedia, respectively. Ethanol (C_2H_5OH), nitric acid (HNO_3), potassium iodide (KI), isopropyl alcohol (IPA), sodium azide (NaN_3) and formic acid (HCOOH) were purchased from Merck. Alizarin red S (C.I. 58005) used as a model pollutant was procured from S.D. fine Chem. Ltd. (India). Commercially available derivatives of titanium dioxide catalyst, PC-50and P25 were obtained from Millennium Inorganic Chemicals, France and Degussa, Germany, respectively. All the solutions were made in highly pure and de-ionized water.

2.2. Catalyst preparation

The TiO_2 colloidal solution was synthesized similar to earlier reported method[10].In a typical synthesis procedure ethanol (60 mL) was added to TTiP (20 mL), to which aqueous ethanolic solution (20 mL water + 40 mL ethanol) was added drop wise. This resulted in formation of a white sol, which was aged for 24 h. With subsequent drying and calcination treatments (450 ˚C for 2 h), TiO_2nanoparticles were synthesized.

An ultrasonic cum sol-gel route was used to prepare Bi^{3+} doped TiO_2. Calculated amount of Bi(III) salt wasadded to appropriate amounts (the molar ratio of Bi:Ti 0.25% to 5%) of ethanol, double distilled water and HNO_3 making a total of 20 mL of reaction mixture volume. This was added slowly drop wise to the prepared TiO_2 sol followed by sustained stirring for 10 h and ultrasonic dispersion for 30 minutes.The obtained products were dried overnight at 80 ˚C and then ground to obtain fine powder. It was further subjected to calcination treatment at 400 ˚C for 2 h. The resultant products were labeled as x% BiT, where x% is Bi/Ti molar ratio.

2.3. Catalyst characterization

The general morphologies of as-prepared catalysts were examined by field emission scanning electron microscopy (FESEM; JEOL-JSM-7600F). The detailed morphological and structural characterizations of the prepared nanoparticles were done by transmission electron microscopy (TEM; JEOL-JEM-2100F) attached with high-resolution TEM (HRTEM). The X-ray diffractograms have been obtained from the X-ray diffraction (XRD; PANanalytical XpertPro.), measured with Cu-Kα Radiation (λ=1.54178Å) in the 2θ range of 10˚-80˚. Fourier transform infrared (FT-IR) spectroscopy was performed by using Thermoscientific (Nicolet iS50) FT-IR spectrometer, equipped with a diamond ATR at room-temperature in the range of 400-4000 cm^{-1}. BET surface area of the samples was analyzed by nitrogen adsorption-desorption in a N_2 adsorption analyzer (NOVA 2000e)USA.Prior to analysis, the samples were degassed at 423K for 5h.The multipoint BET method (adsorption data in relative pressure (P/P_0) range 0.05–0.3) was used to determine the BET surface area. The adsorption isotherm was used to determine the pore-size distribution via the Barret-Joyner-Halender (BJH) method. The pore volume and average pore size was found using the nitrogen adsorption volume at the P/P_0 of 0.994.The room temperature photoluminescence (PL) spectra were measured on Perkin Elmer LS55 fluorescence spectrophotometer using quartz cuvette 1 cm path length. The excitation wavelength applied was of 290 nm. The prepared photocatalysts were also examined by the UV-vis diffuse reflectance spectra (DRS) in the wavelength range of 200–600 nm using a spectrophotometer (Shimadzu UV-2450), with $BaSO_4$ as reference.

2.4. Photocatalytic Experiments

The photocatalytic activities of the Bi-doped TiO_2 nanoparticles were evaluated by the degradation of ARS dye under visible light irradiation (Philips bulb 150 W, Intensity 2150 lm

and wavelength range of 420 nm – 520 nm).For the photocatalytic degradation experiments, different amounts of photocatalyst (Bi-doped TiO_2 nanoparticles) were added into 100 mL of ARS (25 mg/L aqueous solution) and magnetically stirred continuously, so as to maintain homogeneity in the reaction mixture. First, the reaction mixture was stirred in dark for 30 min to obtain adsorption–desorption equilibrium between organic molecules and the catalyst.Then the lights were switched on and the photocatalytic experiments were performed. The samples (3mL) were withdrawn from the reaction mixture, filtered using a Millipore syringe filter of 0.45 μm and analyzed for residual dye concentration remaining in the solution by recording absorption spectra using a Systronics-2202 spectrophotometer. The rate of ARS dye degradation was observed interms of change in intensity at λ_{max}(526 nm) of the dye.The degradationrate (%) was calculated using the equation:

$$\textbf{Degradation rate (\%)} = (C_0 - C)/C_0 \times 100 \qquad (1)$$

Where, C_0 is the initial concentration of dye and C is theconcentration of dye after t (min) of photocatalytic reaction.

3. Results and discussion

In order to synthesize visible light active photo-catalyst, Bi doped TiO_2 nanoparticles (x% BiT) were prepared by an ultrasonic assisted sol-gel method. These were characterized in detail in terms of their crystalline, morphological, compositional, optical, photoluminescent properties, etc. Photocatalytic activity of prepared samples was investigated for the degradation of ARS dye. Further, the role of reactive oxidant species in the photocatalytic degradation reaction was also determined.

3.1. Characterizations and properties of prepared Bi-doped TiO_2 nanoparticles

The crystalline phase and structure of the synthesized x% BiT catalyst were studied by X-ray diffraction. The diffractograms for pure TiO_2 and x% BiT samples are shown in Figure.1. All peaks observed at 25.4˚, 38.1˚, 48˚, 54.1˚, 55.2˚, 62.7, 68.9, 70.5 and 75.2 (2θ) values in the XRD pattern are well matched with anatase (101), (004), (200), (105), (211), (204), (116), (220) and (107) spacing, respectively.This confirms the existence of anatase TiO_2(JCPDS 21-1272) in the samples. The peaks for rutile and brookite were not there in any of the samples. Interestingly, no Bi-doping related peak was observed in the XRD pattern of 0.25% BiT sample due to low-doping content of Bi. However, very weak diffraction peaks corresponding to Bi species could be seen in other BiT samples (0.50, 1 and 3% BiT) because of low dopant concentration. Although significant diffraction peak for Bi species was well observed in 5% BiT sample due to sufficient Bi content in the sample[35,38].

The general morphologies of prepared Bi doped TiO_2 nanoparticles were examined by FESEM (Figure 2). From FESEM images of 0.25% BiTand 0.50% BiT, it was confirmed that the nanoparticles possess almost spherical shape with diameters of ~30 ± 10 nm and ~40 ± 10 nm, respectively (Figure 2(a), (b)). Figure 2 (c) demonstrates the low-magnification and 2 (d) high resolution FESEM image of 1% BiT nanoparticles, which exhibited that the nanoparticles are grown in high-density with the typical diameters of 25 ± 10 nm. Further increase in Bi % leads to agglomeration as seen from the FESEM image of 3% and 5% BiT (Figure 2 (e)-(h)). The diameters of the nanoparticles were found to be ~25 ± 5 nm.

The detailed morphology and structure of prepared BiT nanoparticles were studied by transmission electron microscopy (TEM) along with high-resolution TEM (HRTEM). Figure 3 (a) depicts the TEM image of 1% BiT which are irregular shaped, densely grown nanoparticles.

Considering the morphology and dimensionality, the TEM image is fully consistent with FESEM observations. The HRTEM image shows well-defined lattice fringes (lattice spacing of ~0.35 nm) which shows complete agreement with the distance of [101] crystalline plane of the anatase TiO_2 (Figure 1(b)). Figure 3 (c) shows the TEM image of 3% BiT nanoparticles which reveals slight agglomeration and that the typical diameter of the nanoparticles are ~20 ± 5 nm. The HRTEM image of prepared 3% BiT nanoparticles shows some rough surfaces and defects on the lattice structures which may be due to the addition of Bi^{3+} into TiO_2 crystals (Figure 3 (d)). The observed inter-planar distance between two lattice fringes are ~0.35 nm which corresponds to the [101] orientation of the TiO_2 nanoparticles. Figure 3 (e) illustrates the TEM image of 5% BiT nanoparticles. The observed image is fully consistent with the obtained results of FESEM and confirmed that the diameters of the nanoparticles are ~25 ± 5 nm. Interestingly, much aggregation has been seen in the prepared nanoparticles. Moreover, many defects are seen on the lattices of prepared nanoparticles which are due to the 5% doping of Bi^{3+} into TiO_2 nanoparticles. The observed HRTEM image clearly reveals the lattice spacing of 0.35 nm which corresponds to the (101) crystal planes of the anatase TiO_2 (Figure 3 (f)).

Figure 4 (a) shows FTIR spectrum for bare TiO_2 nanoparticles. The peak at 3366 cm^{-1} corresponds to OH group. The sharp peak at 1629 cm^{-1} is assigned to C=O stretching that can be due to presence of precursor. The peaks at 722 arise due to Ti-O stretching present in TiO_2[10].The characteristic peaks for the 1% BiT sample observed at 3358, 1629 and 746 cm^{-1} were attributed to the presence of OH, C=O and Ti-O in the catalyst, respectively as shown in Figure 4(b). Similar types of spectra were obtained for 3% (Figure 4c) and 5% BiT sample (Figure 4d).

The surface area and the pore structureof the synthesized catalyst were studied by performing N_2 physical adsorption-desorption studies. N_2 adsorption/desorption BET isotherms

and their relative BJH pore size distributions (adsorptionbranch of the isotherms) of 1% BiT sample are depicted in Figure 5. It was found that isotherms are of Type IV, which is typical for mesoporous material according to the IUPAC classification. Table 1 shows the data for surface area, pore volume and pore radius obtained from different methods for 1% BiT catalyst. The 1%BiT sample shows a wide pore size distribution with an average pore diameter at 11 nm (Figure 5 (b)) and the specific surface area of 126.63 m^2/g, which is quite high as compared to the synthesized TiO_2 and widely used TiO_2 P25 (Table 2)[40]. This is because of small particle size of the synthesized catalyst as compared to TiO_2.

The photocatalytic activity of a catalyst is largely determined by the efficiency of the photogenerated electron–hole separation. Since, photoluminescence originates from the recombination of charge carriers; the PL spectra are highly informative to study the recombinations or trapping of charge carriers. Figure6shows the PL spectra for bare TiO_2 and 1%, 3% and 5%BiT samples exhibiting PL emission in the range of 350–500 nm. The characteristic emission peak was observed at 378 nm for bare TiO_2nanoparticles[10]. As compared to sole TiO_2, all the Bi doped TiO_2samplesrevealed a significant reduction in the intensity, which indicates that the BiT samples possess a lower recombination rate of photogenerated charge carriers, thus improved the separation of charge carriers, thereby increasing the quantum efficiency of the photocatalytic reaction. It was observed that 1% and 3% BiT sample exhibited a maximum decrease in PL intensity as compared to 5% BiT sample. As a result, the 1% and 3% BiT samples will be highly helpful in increasing the quantum efficiency of the photocatalytic reaction.

Figure 7 shows the corresponding UV-vis DRS spectra of TiO_2 and x% BiT samples are listed in. The absorption thresholds for the photocatalysts were obtained from the UV–vis DRS

curves by extrapolatingthe tangent lines of the spectra. The band gap energy (E_{bg}) has been calculated using following equation:

$$E_{bg} = 1240/\lambda \qquad (2)$$

As shown in Figure 7(a) the threshold wavelength for the as prepared TiO_2 is 392 nm corresponding to band gap of 3.16 eV.It was observed that the light absorption exhibited significant red-shifts by incorporation of Bi^{3+} ions into TiO_2as shown in Figure 7(b)-(f). Thus, the BiT photocatalysts could hence, be excited by visible light. The presence of Bi extended the threshold wavelength, maximum to 417 nm in 1% BiT sample (Figure 7d). The band gaps calculated for 0.25, 0.5, 1, 3 and 5% BiT were found to be 3.19, 3.18, 2.97, 3.00 and 3.06eV respectively, showing that the optimal Bi dopant content was 1% which led to a maximum extension of spectral wavelength into visible region. The extension towards visible light region is because of Bi^{3+} doping. Since, there is reduction of band gap; the energy band has beenproposed to lie between Bi^{3+} 6s band and Ti^{4+} 3d band[41]. Thus,a significant red shift is observed which leads to the absorption of lower energy photons lying in the visible spectral range.

3.2. Photocatalytic properties of prepared Bi-doped TiO_2 nanoparticles

The catalytic activity of x% BiT catalysts was determined by conducting experiments for photocatalytic degradation of ARS dye, under visible light illumination. The optimum amount of catalyst dose and molar concentration of Bi dopant required for the photocatalytic reaction were also examined.

a) Effect of Bi doping

Figure 8 (a) shows the absorption spectra of photo-degradation of ARS dye under visible irradiation with 1% BiT catalyst. Since ARS exhibits absorptionband around 526 nm, bare TiO_2

degraded 50% of ARSbecause of dye sensitization[42]. The catalytic activities were found to increase as the molar ratio Bi:Ti was increased from 0% to 5%. This enhancement in photocatalytic activity upon doping TiO_2 with Bi^{3+} maybe attributed to high specific surface area, the inhibitionof electron and hole recombination by the Bi species doped in $TiO_2$and the increase in absorption of visible light as illustrated in BET isotherms, PL spectra and UV-vis DRS, respectively. As expected, maximum degradation rate was observed with 1% BiT catalyst, where ARS was 82% degraded within 90 min (Figure 8(b))because of maximum extension of spectral response into visible region and suppression of electron and holes recombination. The comparatively lesser red shift in the 0.25, 0.5, 3and 5% BiT sample as compared to the 1% BiT sample further explains the reason why they show lesser degradation efficiency as compared to the 1% and 3% BiT phtocatalyst.

b) Optimum catalyst dose

The optimum catalyst dose was determined by carrying out photocatalytic degradation of ARS dye in aqueous phase with varied doses of BiT catalysts from 0.025 g/L to 0.2 g/L under similar experimental conditions. This was done to ensure the use of minimum required amount of catalyst and maximize the absorption of photons for the catalytic process. In the absence of catalyst; no detectable degradation of dye was observed (Figure 9(a)). Figure 9 (b) shows the effect of catalyst loading on percentage degradation of ARS dye under visible light illumination. It was observed that with increasing catalyst dose up to 0.1 g/L, the rate of photo-degradationshows marked increase, thereafter the rate of degradation decreases. The initial increase in the catalytic activity is because of increase in the total active surface area and active sites upon addition of catalyst. Further, at higher catalyst dose, decrease in percentage

degradationis due to deactivation of active molecules caused by collisions with the ground state moleculesand also hindrance to the photons reaching the active surface sites caused by the presence excess molecules[3, 6].

c) Comparison with other photocatalysts

To demonstrate the superior photocatalytic activity of the prepared photocatalysts as compared to other commercially available photocatalysts, a set of photocatalytic experiments were performed under similar conditions using TiO_2(PC-50) and TiO_2 (P25) as commercial photocatalysts. The plot of C_i/C_0(where C_i and C_0refer to dye concentration at time (t) and initially at time (t=0), respectively) versus time depicting the extent of photo-degradation of ARS using the synthesized and commercial photocatalysts has been shown in Figure 10 (a). It was observed that with increase in time the relative concentration of dye decreasesbut a maximum decrease was observed with 1% BiT catalyst. Also, the percentage degradation rates have been compared for the catalysts (Figure 10 (b)). The commercial TiO_2 photocatalysts (PC-50, P25) show only 30-40% degradation rate for ARS dye under similar conditions. It is clear that the prepared photocatalysts, viz. x% BiT exhibit much higher degradation efficiency as compared to other photocatalysts, which can be credited to the presence of anatase crystalline phase of TiO_2, high surface area, extension of the absorption of TiO_2 into visible light region and inhibition of electron-hole recombinations due to doping of Bi into TiO_2.

d) Kinetics study

The reaction kinetics of photocatalytic degradation of ARS dye (25 mg/L) under optimum conditions was also studied. It was found that the ARS photodegradation follows 1st order Langmuir Hinshelwood equation:

$$\ln C_0/C_i = kt, \qquad (3)$$

The graph was plotted between ln C_0/C_i vs t as shown in Fig.11. The correlation constant for the fitted line was found to be $R^2 = 0.9811$ and the reaction rate constant k was found to be 0.0232 min^{-1}.

e) The role of reactive oxygen species:

The photocatalytic oxidation reactions involving TiO_2 comprise of certain reactive oxygen species (ROSs) and it is important to determine role of these ROSs. Quencher chemicals can be used to find which reactive oxygen species plays an important role during the photocatalysis. So, to investigate the role of these reactive species, different scavengers were added to the reaction mixture to study their inhibitory effects. As shown in Figure12, the maximum degradation of ARS dye was achieved in absence of any quencher species, because of conjunctive role of the ROSs generated during the photocatalytic reaction. In order to study the role of •OH, IPA was added into the reaction mixture.[43,44] Addition of IPA significantly reduced the degradation process, thereby proving that •OH is expository for TiO_2photocatalysis. When sodium azide (quencher for singlet oxygen ($^1O_2$) and •OH) was added, similar quenching effects were observed, suggesting that $^1O_2$ does not impart much contribution in the degradation process.[45,46]

Further, the role of hole in photo-degradation was investigated by addition of formic acid which acts as sacrificial electron donor.[47] It was found that only a feeble decrease in degradation took place. However, in the presence of KI, (scavenger for holes and •OH) there was significant reduction in degradation process, implying that •OH are major species involved in the photocatalytic degradation process.[48-50]

f) Proposed mechanism

The earlier studies have proposed that the Bi^{3+}(6s)level is very important in reducing the energy band gap of TiO_2, which lies between the Bi^{3+} 6s band and Ti^{4+} 3d band. This leads to absorption of lower energy photons, leading to enhancement in photocatalytic quantum efficiency.[41,51] The following reaction sequence shows the plausible mechanism of reaction on the surface of Bi-doped TiO_2photocatalyst:

$$BiT \xrightarrow{h\nu} Bi^{3+}_{6s}(h^+) + TiO_2(e^-)$$

$$OH^- + h^+ \rightarrow HO^\bullet$$

$$O_2 + e^- \rightarrow O_2^{\bullet-}$$

$$O_2^{\bullet-} + H^+ \rightarrow HO_2^\bullet$$

$$HO_2^\bullet + e^- \rightarrow HO_2^-$$

$$HO_2^- + H^+ \rightarrow H_2O_2$$

$$H_2O_2 + e^- \rightarrow OH^- + HO^\bullet$$

$$ARS + HO^\bullet \rightarrow CO_2 + H_2O + \text{simple molecules}$$

When the BiT photocatalyst is illuminated, a photon of energy higher or equal to the band gap ($h\nu \geq E_{bg}$), causes excitation of electrons into the conduction band (CB) of TiO_2.

Simultaneously, equal number of holes are generated in the 6s level of Bi^{3+} (Figure11). The electrons are then taken up by the adsorbed O_2 present on the surface of TiO_2 generating $O_2^{\bullet-}$.[52] The subsequent reactions of OH^- and $O_2^{\bullet-}$ can also generate highly oxidizing species, hydroxyl radicals ($HO^{\bullet}$) which degrade the organic moiety (ARS) completely into simpler molecules.[35, 52-54]

4. Conclusions

TiO_2 nanoparticles doped with varied molar concentrations of bismuth were successfully synthesized by a sol–gel method. The synthesis route followed lead to formation of crystalline anatase TiO_2 nanoparticles with excellent optical and photoluminescent characteristics. It was found that the incorporation of Bi^{3+} ions in TiO_2 lattice lead to significant improvement in photocatalytic degradation rate of ARS dye, primarily because of high surface area and itlead to the extension of absorption of TiO_2 into visible light region and efficient separation of charge carriers. However, the degradation efficiency depended upon the Bi^{+3} ion doping concentration and dose of the prepared catalyst. TiO_2 doped with 1% Bi^{+3} ion doping concentration and 0.1 g/L dose exhibited best photocatalytic degradation efficiencies for the dye. Therefore, it can be concluded that Bi-doped TiO_2 nanoparticles are promising photocatalysts which may be used for the wastewater remediation on industrial scale.

Acknowledgments

The authors greatly acknowledge the financial support received under the UGC (Major Project), Government of India through a project grant F. No. 41-364/2012(SR) and TEQIP-II grant of Dr. S.S. Bhatnagar UICET, Panjab University, Chandigarh. Ahmad Umar would like to

acknowledge the support of the Ministry of Higher Education, Kingdom of Saudi Arabia through a grant (PCSED-001-11) under the Promising Centre for Sensors and Electronic Devices (PCSED) at Najran University, Kingdom of Saudi Arabia.

References

[1]M. Schiavello, Heterogeneous photocatalysis, John Wiley & Sons, England, 1997.

[2] (a) S.K. Kansal, R. Lamba, S.K. Mehta and A. Umar, *Mater. Lett.*, 2013, **106**, 385; (b) L. Liu, Y. Cao, J. He, X. Qi, W. Shi, and Q. Yang, *J. Nanosci. Nanotechnol*. 2013, **13**, 6835-6840

[3](a) S.K. Kansal, N. Kaur and S. Singh, *NanoscaleRes. Lett.,*2009, **4**, 709; (b) S. Xu and D. D. Sun*, J. Nanosci. Nanotechnol*. 2013, **13**, 6866-6871

[4](a) S. D. Hwang, S. W. Kim, W. K. Lee, E. J. Kim, and S. H. Hahn, *J. Nanosci. Nanotechnol*. 2013, **13**, 7059-7061; (b) C. Yang, W. Huang, T. Huang and H. Huang, *Sci. Adv. Mater*., 2014, **6**, 9-17; (c) X. Cheng, G. Pan, X. Yu, T. Zheng, Ahmad Umar, and Q. Wang*, J. Nanosci. Nanotechnol*. 2013, **13**, 5580-5585

[5] (a) A.D. Paola, E.G. López, G. Marcì and L. Palmisano**,** *J. Hazard. Mater.,*2012, **211– 212**, 3; (b) H. Kim and K. Lee*, J. Nanosci. Nanotechnol*. 2013, **13**, 5597-5600

[6] (a) S.K. Kansal, A.H. Ali and S. Kapoor, *Desalinatio*n, 2010,**259**, 147; (b) H. Feng, M.-H. Zhang, and L. E. Yu, *J. Nanosci. Nanotechnol*. 2013, **13**, 4981-4989; (c) A. T. Kuvarega, R. W. M. Krause, and B. B. Mamba*, J. Nanosci. Nanotechnol*. 2013, **13**, 5017-5027

[7](a) S.S. Arbuj, N. Rumale, A. Pokle, J. D. Ambekar, S. B. Rane, U. P. Mulik and D.P.Amalnerkar, *Sci. Adv. Mater.,*2014, **6,** 269; (b) S. K. Kansal, Mani, H. Kumar, Ahmad Umar, and W. Deng, *J. Nanosci. Nanotechnol*. 2013,**13**, 4172-4177

[8](a) C. Burda, Y. Lou, X. Chen, A. Samia, J. Stout and J. Gole, *Nano Lett.*, 2003, **3**, 1049; (b) B. Palanisamy, C. M. Babu, B. Sundaravel, S. Anandan, and V. Murugesan, *J. Nanosci. Nanotechnol*. 2013, **13**, 2573-2581

[9](a) V. Kozhukharov, P. Vitanov and P. Stefchev, *J. Environ. Prot. Ecol.*, 2001, **2**, 107; (b) P. Namkhang, W.-J. An, W.-N. Wang, K. S. Rane, P. Kongkachuichay, and P. Biswas*, J. Nanosci. Nanotechnol*. 2013, **13**, 2376-2381

[10] (a) S.K. Kansal, S.Sood, A. Umar and S.K. Mehta, *J. Alloys Compd.,*2013, **581,** 392; (b) L.-S. Zhang, W.-F. Lin, M.-Q. Xia, L.-H. Leng, G.-X. Chen, J.-P. Zou, L. Zhong, X.-Y. Wei, M.-M. Lu, M.-X. Li, X.-M. Tu, and S.-L. Luo*, Sci. Adv. Mater*. 2014, **6**, 853-861

[11] (a) A. Fujishima, T.N. Rao and D.A. Tryk, *J. Photochem. Photobiol. C,*2000, **1**, 1.; (b) P. Jing, W. Lan, Q. Su, M. Yu, and E. Xie, *Sci. Adv. Mater*. 2014, **6**, 434-440

[12] (a) W. Zhou, D. Wang, H. Liu, and J. Wang, *Sci. Adv. Mater*. 2014, **6**, 538-544; (b) H. Einaga, S. Futamura and T. Ibusuki, *Appl. Catal. B,*2002, **38,** 215

[13] (a) S. K. Kansal, G. Kaur and S. Singh, *React.Kinet.Catal.Lett.*, 2009, **98**, 177; (b) F. Deng, K. Li, X. Luo, S. Luo, G. Zeng, S. Wu, and C. Au, *Sci. Adv. Mater*. 2014, **6**, 577-585

[14] X. Cheng, H. Liu, X. Yu, Q. Chen, J. Li, P. Wang, A. Umar and Q. Wang, Sci. *Adv. Mater.*, 2013, **5**, 1563

[15] M. Zhang, S. Shi, G. He, X. Song and Z. Sun,*Sci. Adv. Mater.,*2014, **6**, 170

[16] T. K. Ghorai, M. Chakraborty and P.Pramanik, *J. Alloys Compd.*,2011, **509**, 8158

[17] M. A. Ahmed, *J. Photochem. Photobiol. A*, 2012, **238**, 63

[18] M. Shao, X. Xu, J. Huang, Q. Zhang and L. Ma,*Sci. Adv. Mater*., 2013,**5**, 962

[19] Y.C. Nah, A. Ghicov, D. Kim, S. Berger and P. Schmuki, *J. Am. Chem. Soc*., 2008, **130**, 16154

[20] N. Naseri, M. Yousefi and A.Z. Moshfegh, *Sol. Energ.,*2011, **85**, 1972

[21] Q. Li, L. Zong, Y. Xing, X. Wang, L. Yu andJ.Yang, *Sci. Adv. Mater*., 2013,**5**, 1316

[22] R. Asahi, T. Morikawa, T. Ohwaki, K. Aoki and Y. Taga, *Science*, 2011, **293**, 269

[23] J.L. Gole, J.D. Stout, C. Burda, Y. Lou and X. Chen,*J Phys. Chem. B,* 2004,**108,** 1230

[24] Y. Yu, J. C. Yu, C. Y. Chan, Y.K. Che, J.C. Zhao, L. Ding, W.K. Ge and P.K. Wong, *Appl. Catal. B,* 2005,**61,** 1

[25] T. Ohno, M. Akiyoshi, T.Umebayashi, K. Asai, T. Mitsui and M. Matsumur,*Appl. Catal. A*, 2004, **265**, 115

[26] S. Tieng, A. Kanaev and K. Chhor, *Appl. Catal. A*,2011, **399**, 191

[27] H. Yamashita, M. Harada, J. Misaka, M. Takeuchi, K. Ikeue andM. Anpo, *J. Photochem. Photobiol. A,* 2002, **148**, 257

[28] S. Liu, G. Wang, Y. Li andL.Meng,*Sci. Adv. Mater*., 2014, **6**, 361

[29] X.C. Wang, K. Maeda, X.F. Chen, K. Takanabe, K. Domen, Y.D. Hou, X.Z. Fu and M. Antonietti, *J. Am. Chem. Soc.,* 2009, **131**, 1680

[30] C.J. Wu and C.H. Chen, *J. Photochem. Photobiol. A*, 2004, **163**, 509.

[31] S. Murcia-López, M.C. Hidalgo and J.A. Navío, *Appl. Catal. A,* 2011, **404**, 59

[32] J. Xu, W. Wang, M. Shang, E. Gao, Z. Zhang and J. Ren, *J. Hazard. Mater*., 2011, **196**, 426

[33] Y. Hu, Y. Cao, P. Wang, D. Li, W. Chen, Y. He, X. Fu, Y. Shao and Y. Zheng, *Appl. Catal. B,* 2012, **125**, 294.

[34] S. Bagwasi, Y. Niu, M. Nasir, B. Tian and J. Zhang, *Appl. Surf. Sci.,* 2013, **264**, 139

[35] J. Wang, L. Jing, L. Xue, Y. Qu and H. Fu, *J. Hazard. Mater.,* 2008, **160**, 208

[36] J. Hou, Z. Wang, S. Jiao and H. Zhu, *J. Hazard. Mater.,* 2011,**192**, 1772

[37] T. Ji, F. Yang, Y. Lv, J. Zhou and J. Sun, *Mater. Lett*., 2009, **63**, 2044

[38] P.A.K. Reddy, B.Srinivas, P. Kala, V. D.Kumari and M. Subrahmanyam, *Mater. Res. Bull.*, 2011, **46**, 1766

[39] J. Xu, M. Chen and D. Fu, *Appl. Surf. Sci*., 2011,**257**, 7381

[40] X. Cheng, X. Yu and Z. *Xing, J. Phys. Chem. Solids*, 2013, **74**,684

[41] W.F. Yao, H. Wang, X.H. Xu and X.F.Cheng, J. Huang, S.X. Shang, X. N. Yang, M. Wang, *Appl. Catal. A*(2003), **243**, 185

[42] C.C. Chen, W.H. Ma and J.C. Zhao, *Chem. Soc. Rev.*, 2010, **39**, 4206

[43] C. Minero, G. Mariella, V. Maurino, D. Vione and E. Pelizzetti, *Langmuir*, 2000, **16**, 8964

[44] A. A. Khodja, A. Boulkamh and C. Richard, *Appl. Catal. B: Environ.* 2005, **59**, 147

[45] S. Zheng, Y. Cai and K.E. O'Shea, *J. Photochem. Photobiol. A: Chem.* 2010, **210**, 61.

[46] S. Zheng, W. Jiang, Y. Cai, D. D. Dionysiou, K. E. O'Shea,*Catal. Today*, 2014, **224**, 83.

[47] S. Rengaraj and X.Z. Li, *Chemosphere*, 2007, **66**, 930–938

[48] J. Rabani, K. Yamashita, K. Ushida, J. Stark and A. Kira, *J. Phys. Chem. B*, 1998, **102**, 1689

[49] T. An, J. An, H. Yang, G. Li , H. Feng, X. Nie, *J. Hazard. Mater.*, 2011, **197**, 229.

[50] X. Zhang, D.D. Sun, G. Li, Y. Wang, *J. Photochem. Photobiol. A, Chem.*, 2008, **199**, 311

[51] H. Mizoguchi, K. Ueda, H. Kawazoe, H. Hosono, T. Omata and S. Fujitsu, *J. Mater. Chem.,* 1997, **7**, 943

[52] J. Yang, C.C. Chen, H.W. Ji, W.H. Ma and J.C. Zhao, *J. Phys. Chem. B*, 2005, **109,** 21900

[53] L.R. Zheng, Y.H. Zheng, C.Q. Chen, Y.Y. Zhan, X.Y. Lin, Q. Zheng, K.M. Wei and J.F. Zhu,*Inorg. Chem.,* 2009, 48, 1819

[54] N. A. Mir, A. Khan, K. Umar and M. Muneer, *Energy Environ. Focus*, 2013, **2**, 208

Figure captions

Fig.1. XRD pattern of bare TiO_2 and x% BiT samples where, * indexed for anatase phase of TiO_2 and # depicts diffraction peaks for bismuth doped species.

Fig.2. FESEM images of (a) 0.25% BiT; (b) 0.50% BiT; (c), (d) 1% BiT; (e),(f) 3% BiT and (g), (h) 5% BiT samples.

Fig.3. TEM and HRTEM images of (a), (b)1% BiT; (c),(d) 3% BiT and (e), (f) 5% BiT samples.

Fig.4. FTIR spectra of (a) bare TiO_2 nanoparticles; (b) 1% BiT; (c) 3% BiT and (d) 5% BiT

Fig.5.(a)N_2 adsorption–desorption BET isotherm; (b) BJH pore size distributions (from the adsorptionbranch of the isotherms)of 1% BiT photocatalyst.

Fig.6. Room temperature PL spectra of bare TiO_2, 1%, 3% and 5% BiT samples at an excitation wavelength of 290 nm.

Fig.7.UV–vis DRS spectra with band gap extrapolation lines for (a) bare TiO_2; (b) 0.25% BiT; (c) 0.50% BiT; (d) 1% BiT; (e) 3% BiT and (f) 5% BiT sample.

Fig.8.(a) UV–vis absorbance spectra of visible light induced degradation of ARS dye aqueous solution (25 mg/L), (1% BiT, catalyst dose: 0.1 g/L, pH: 7.2), inset shows the molecular structure of ARS dye; (b) Effect of Bi doping on % degradation rate of ARS dye

Fig.9.(a)Comparison of photocatalysis and photolysis; (b) Effect of catalyst dose on % degradation rate of ARS dye.

Fig.10. (a) The extent of degradation of ARS dye with different photocatalysts; (b) Comparison of % photodegradation of ARS dye aqueous solution using synthesized catalysts with those of commercial catalysts (ARS dye concentration 25 mg/Lcatalyst dose: 0.1 g/L, pH: 7.2, time: 90 minutes)

Fig.11. Plot of ln C_0/C_ivs t depecting ARS photodegradation follows 1st order kinetics.

Fig. 12 (a)The extent of degradation and (b) Comparison of % photodegradation rate of ARS dye aqueous solution (25 mg/L) using 1% BiT catalyst with and without scavengers

Fig.13. Mechanism of photocatalytic reaction

Figures

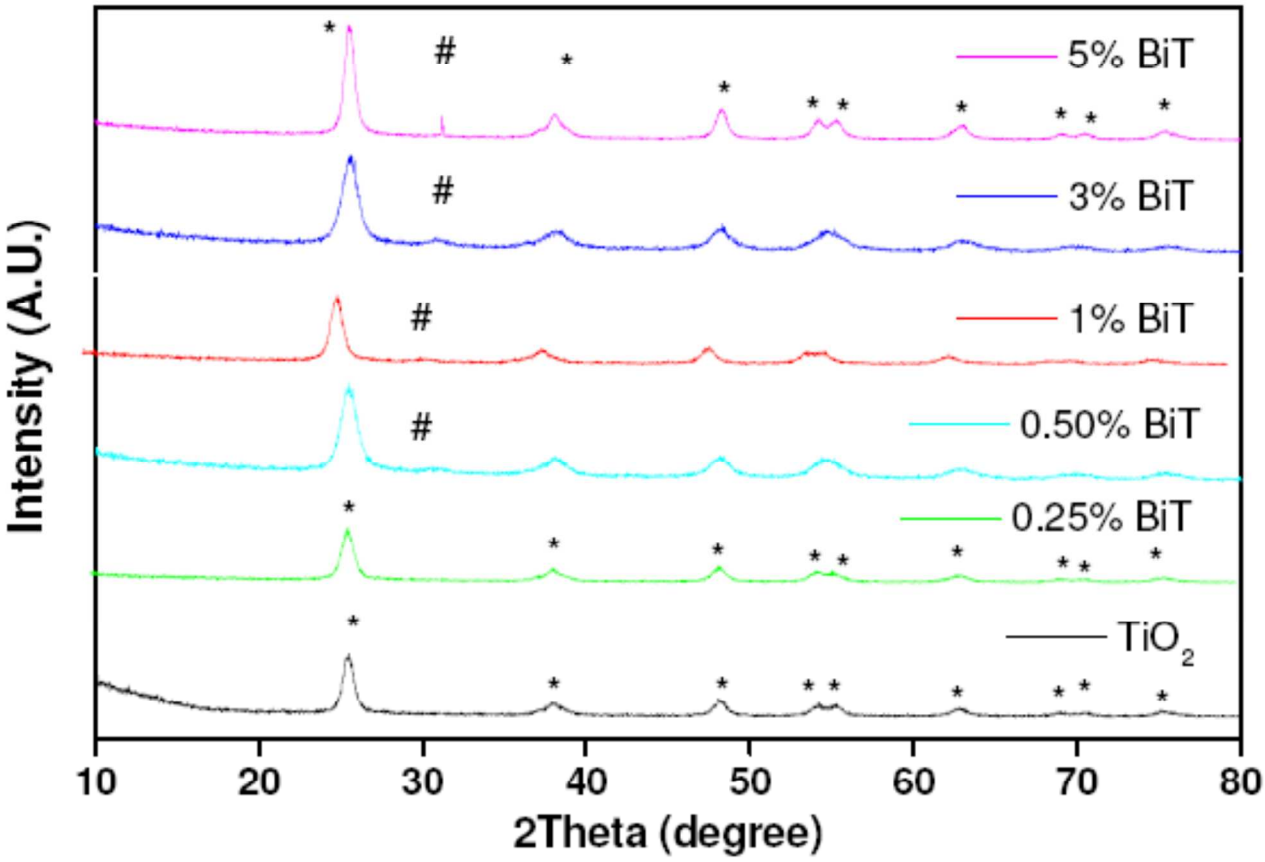

Figure-1

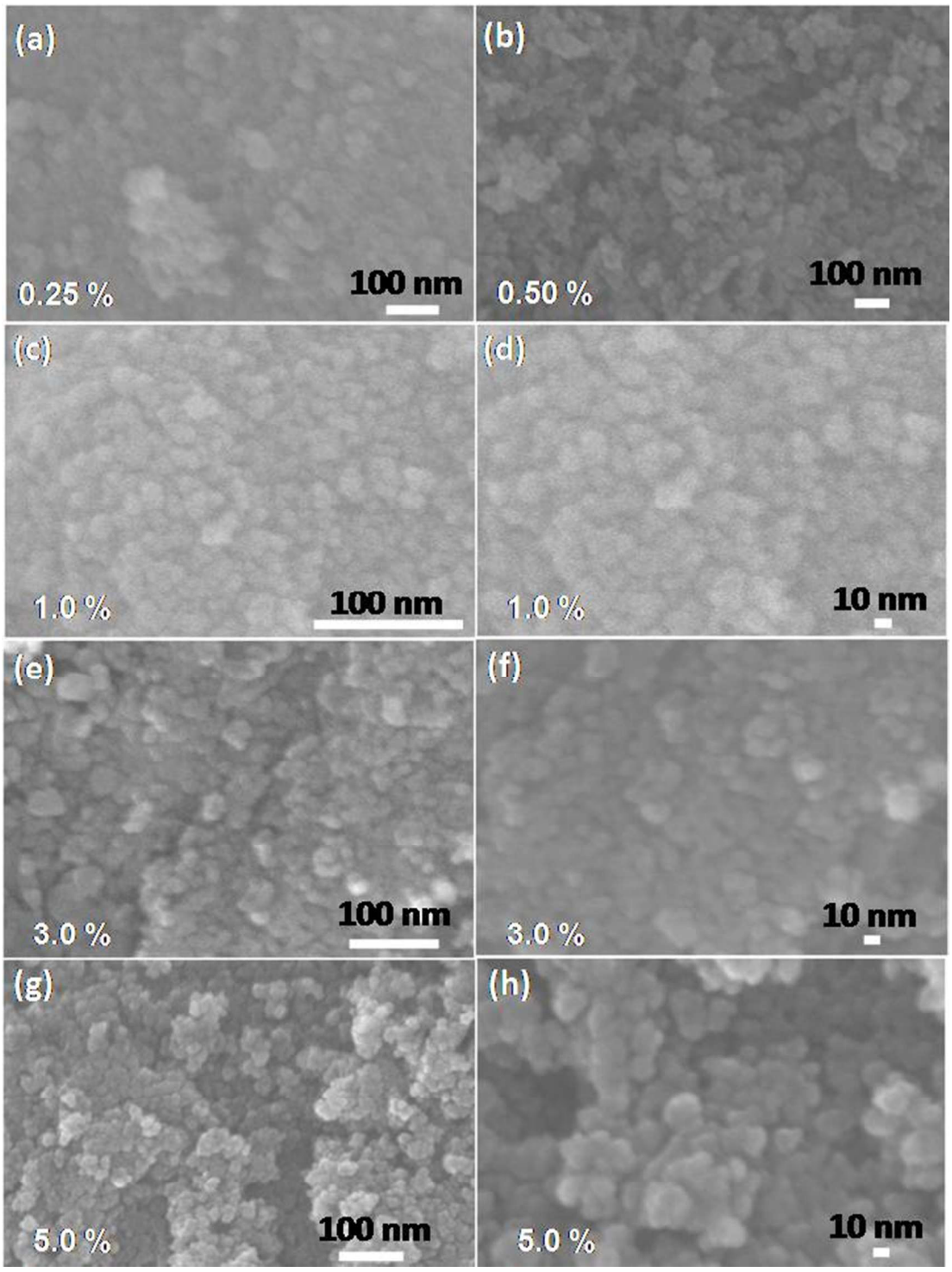

Figure-2

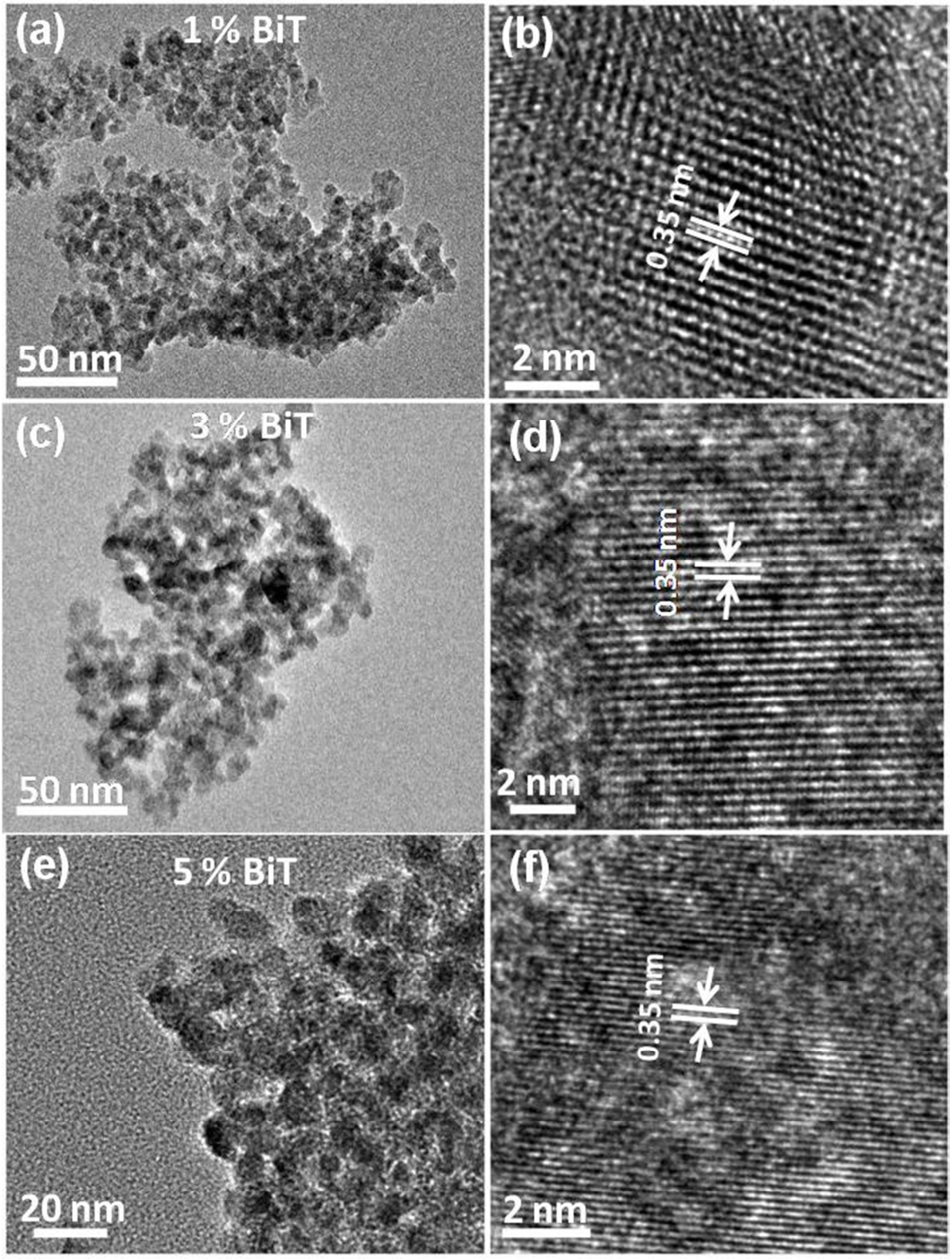

Figure-3

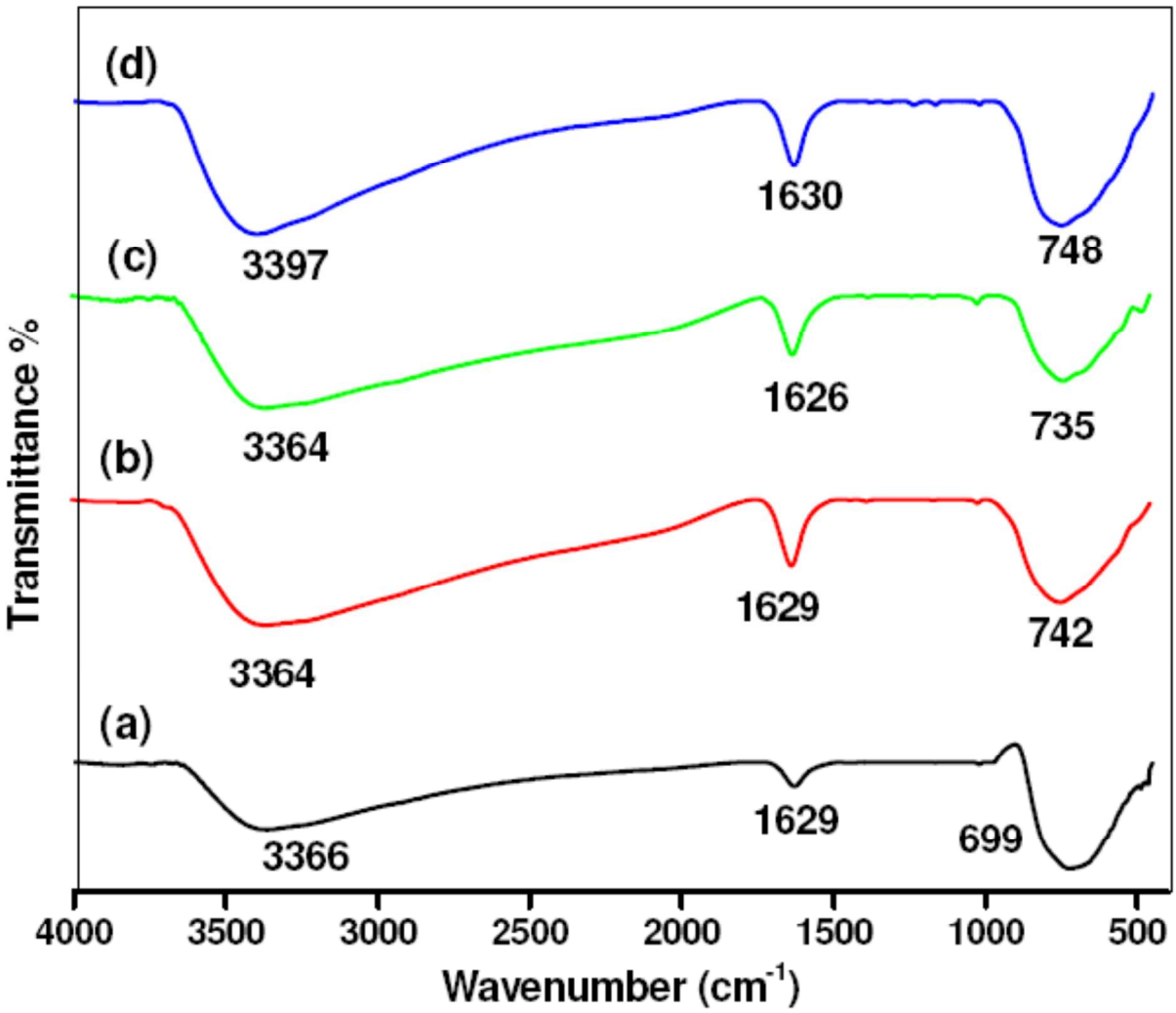

Figure-4

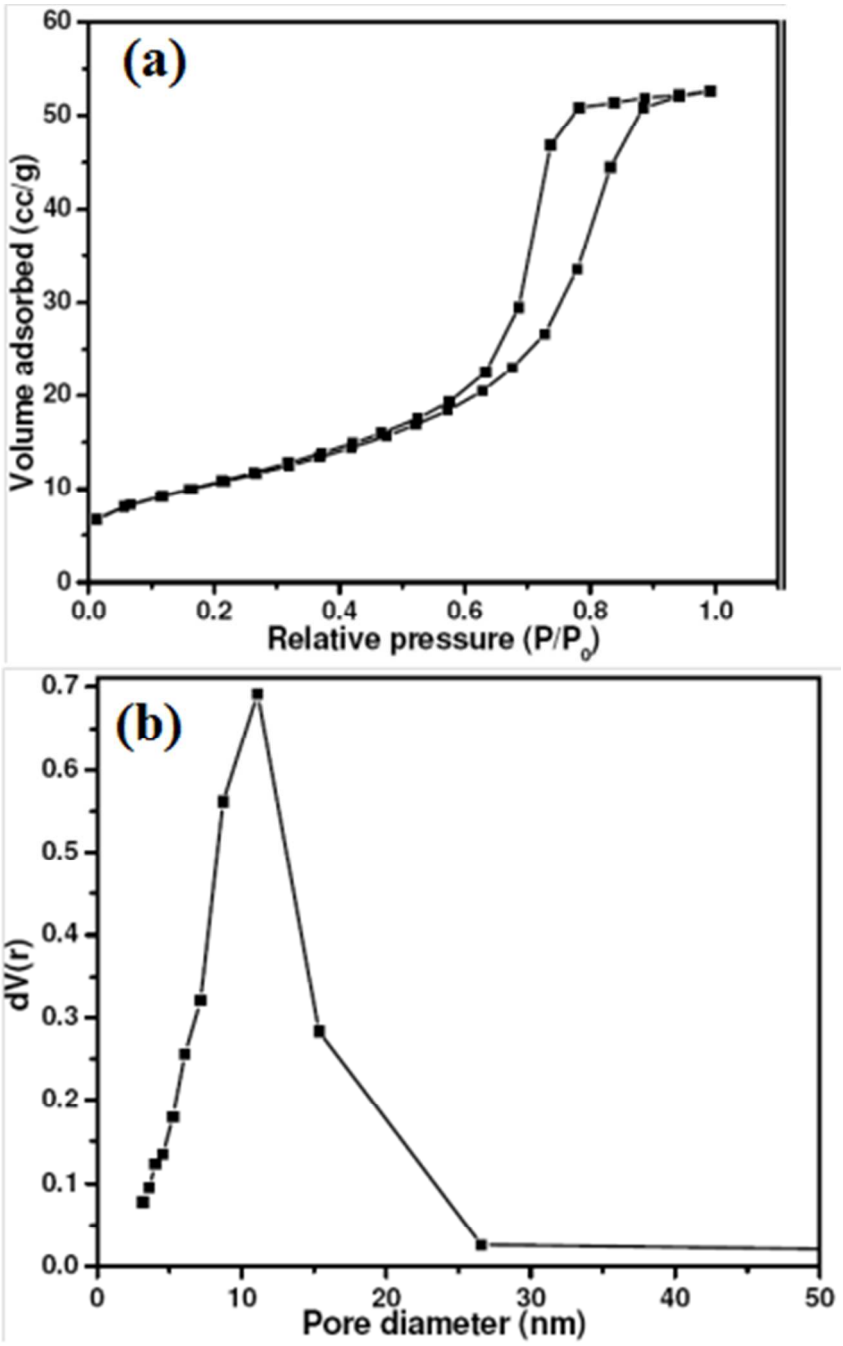

Figure 5

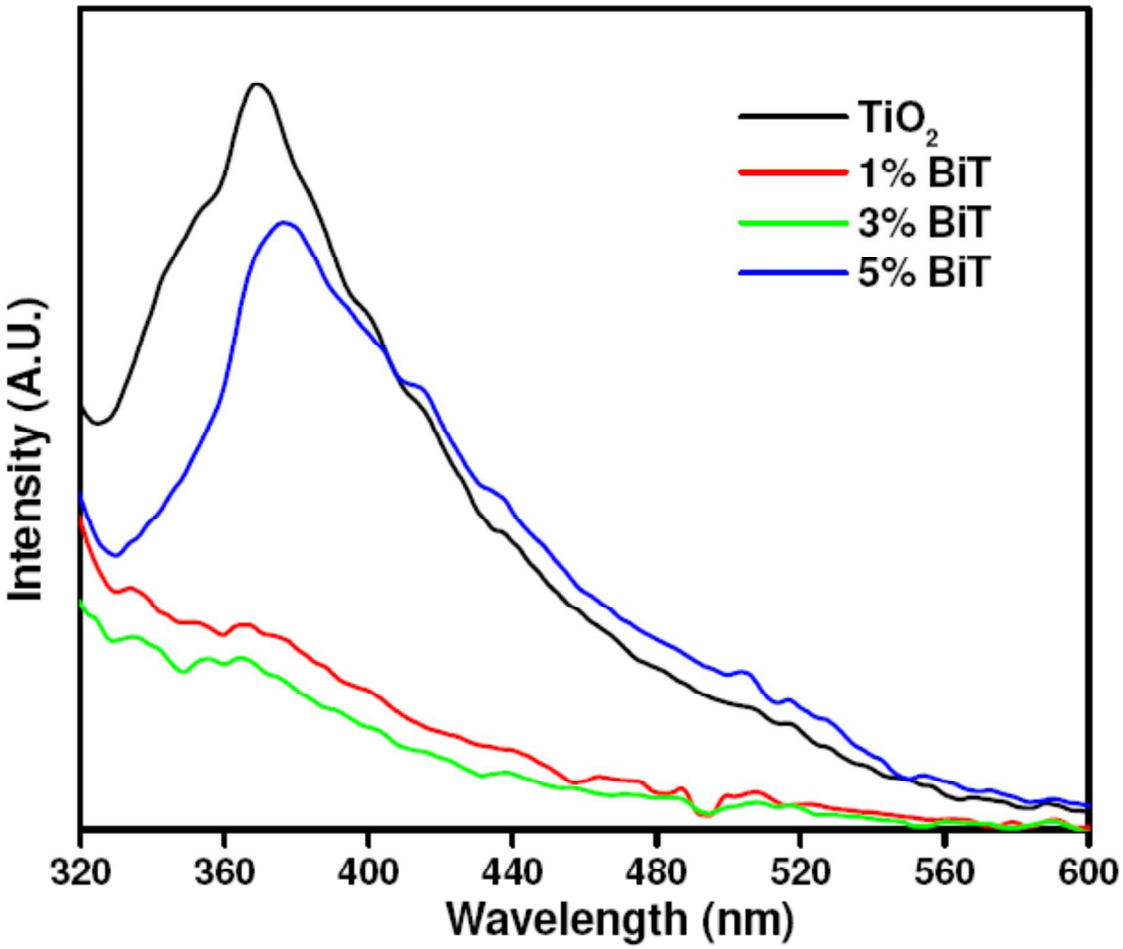

Figure-6

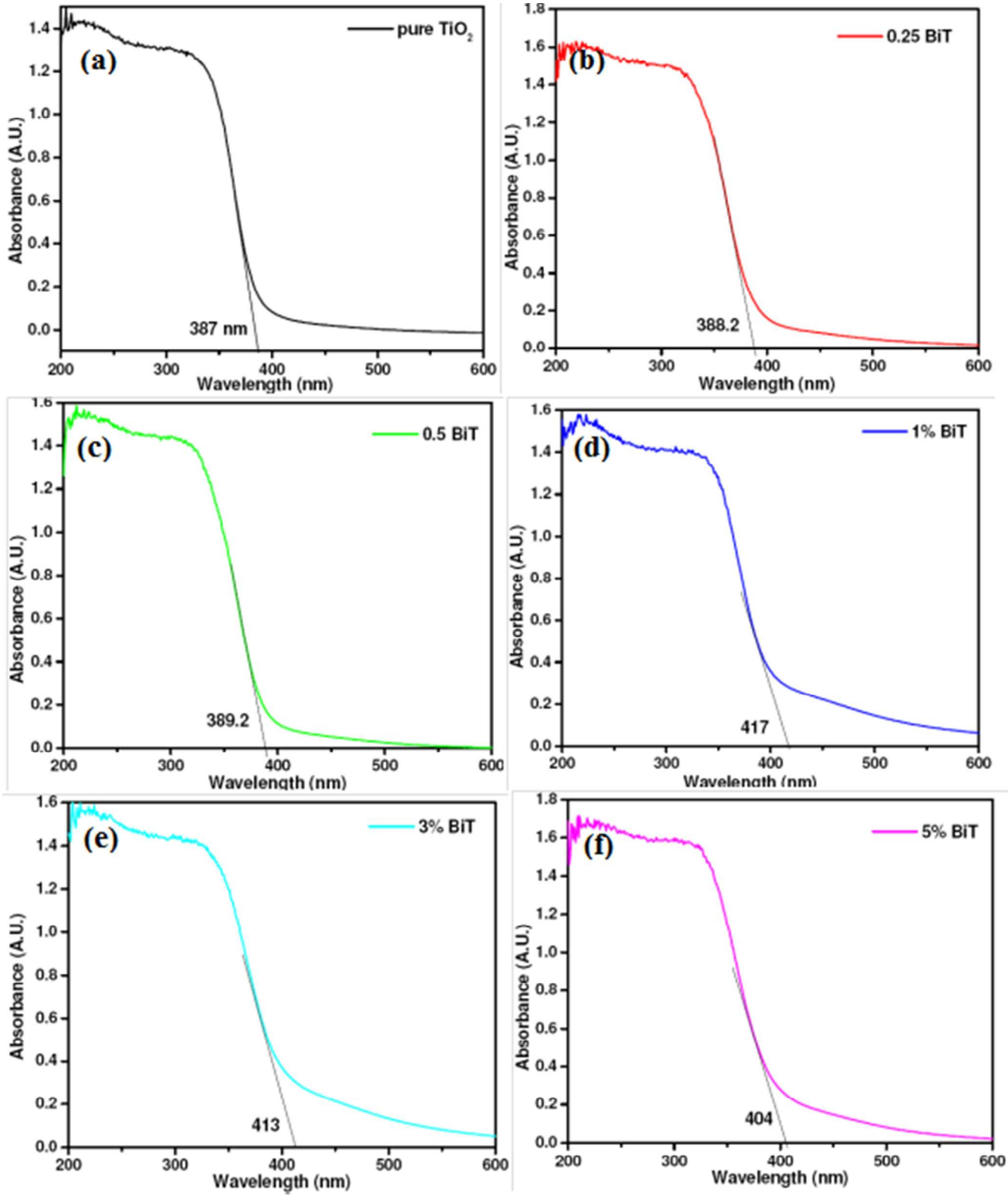

Figure-7

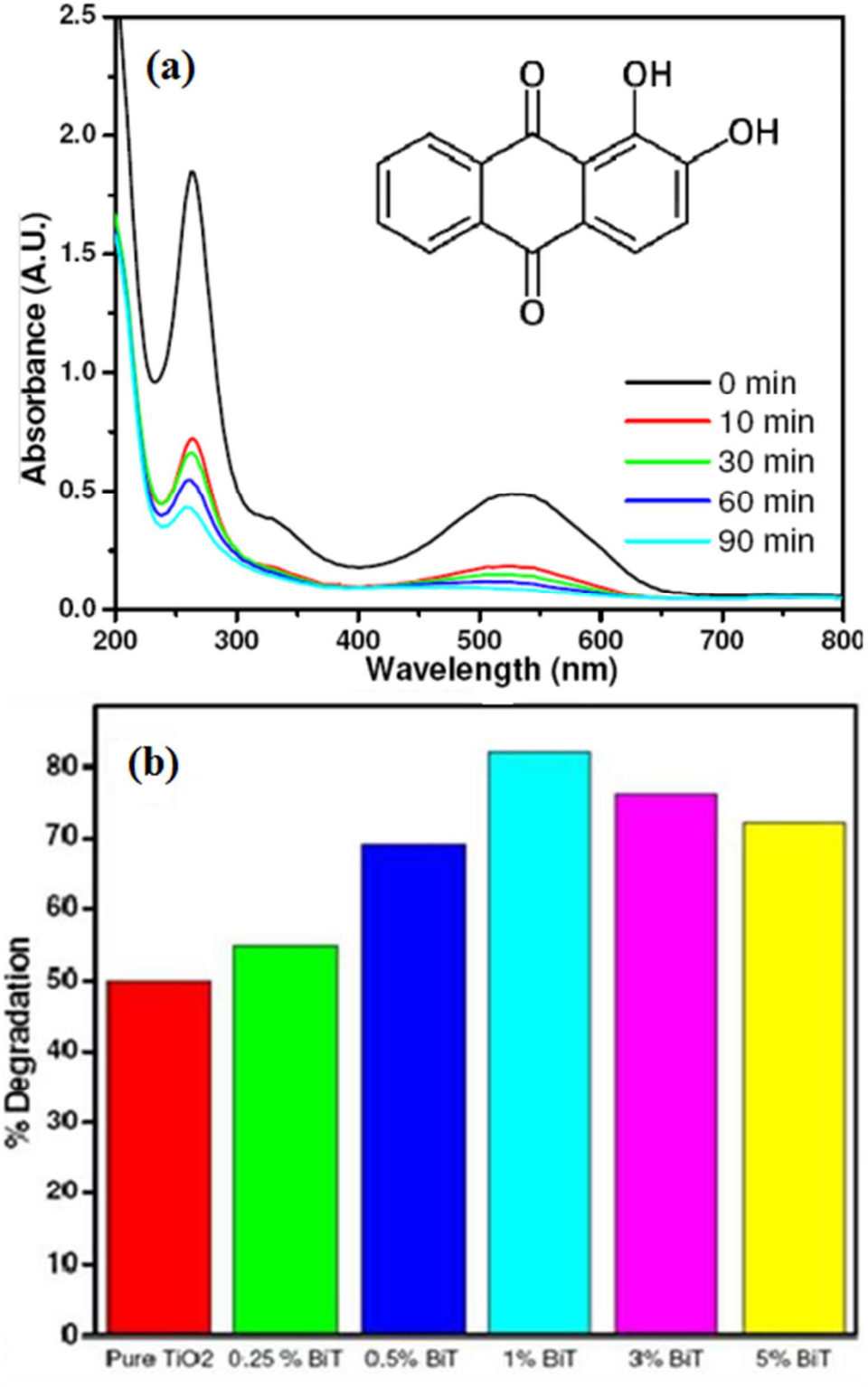

Figure-8

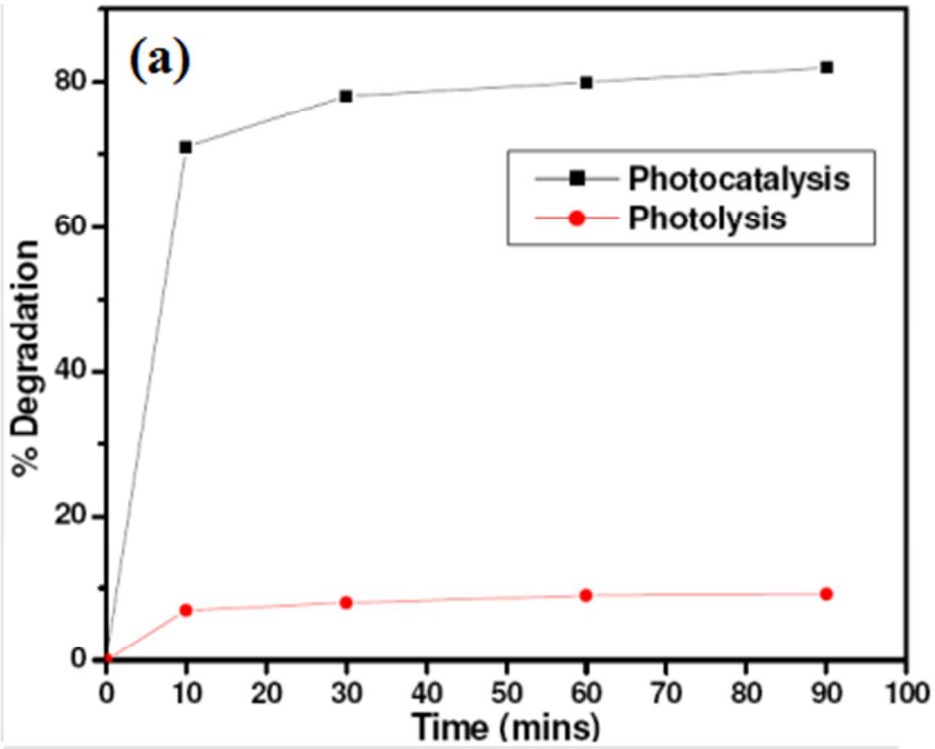

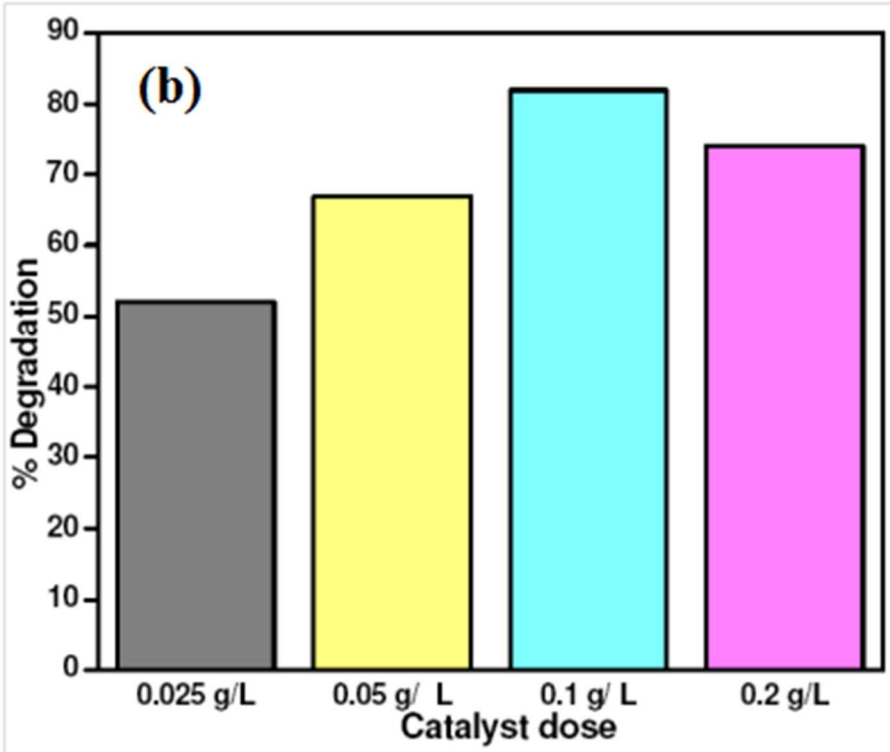

Figure-9

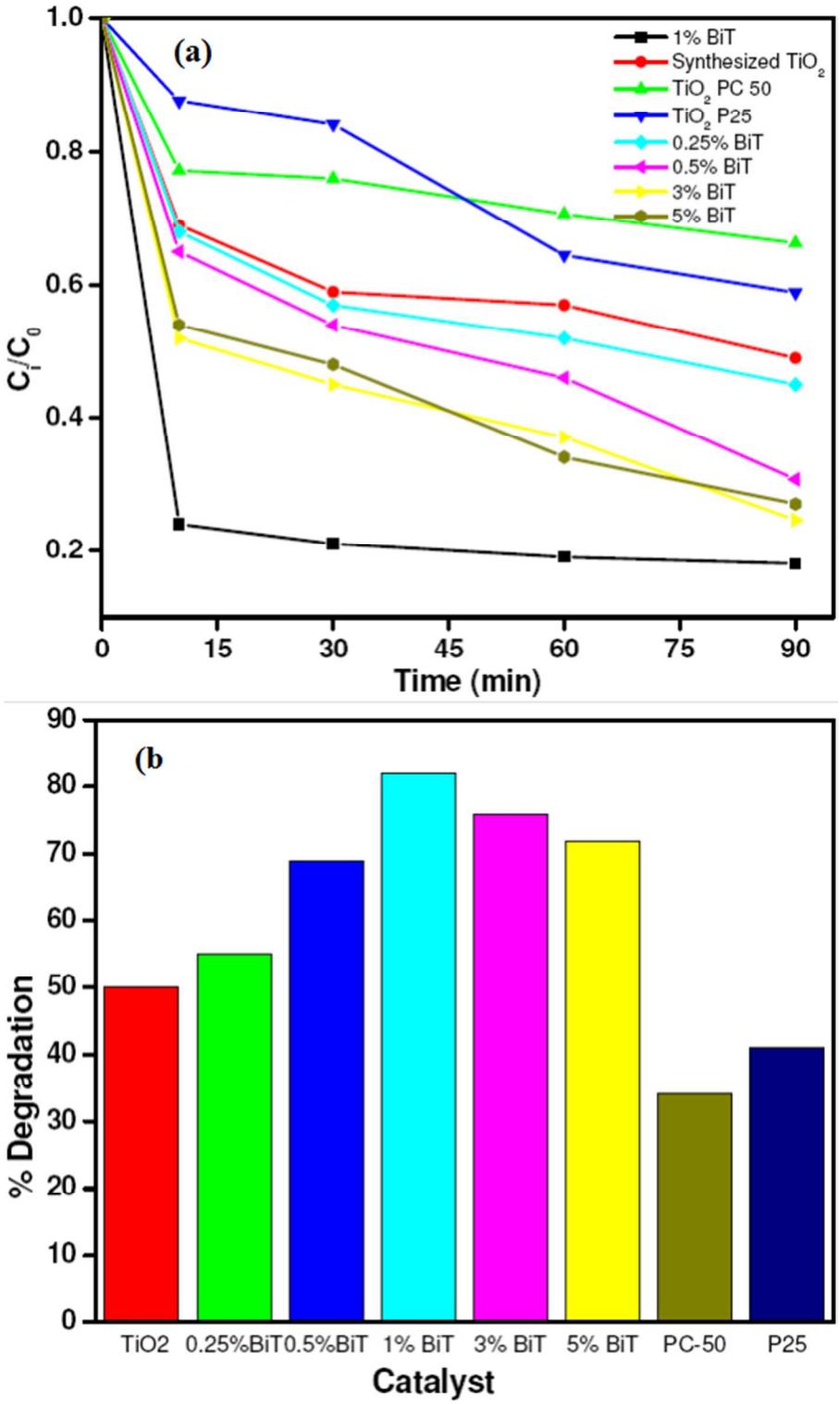

Figure-10

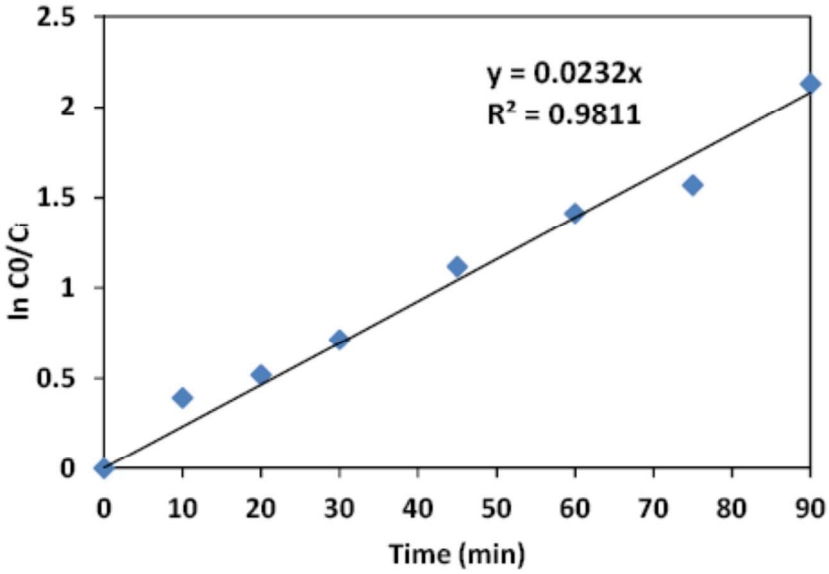

Figure-11

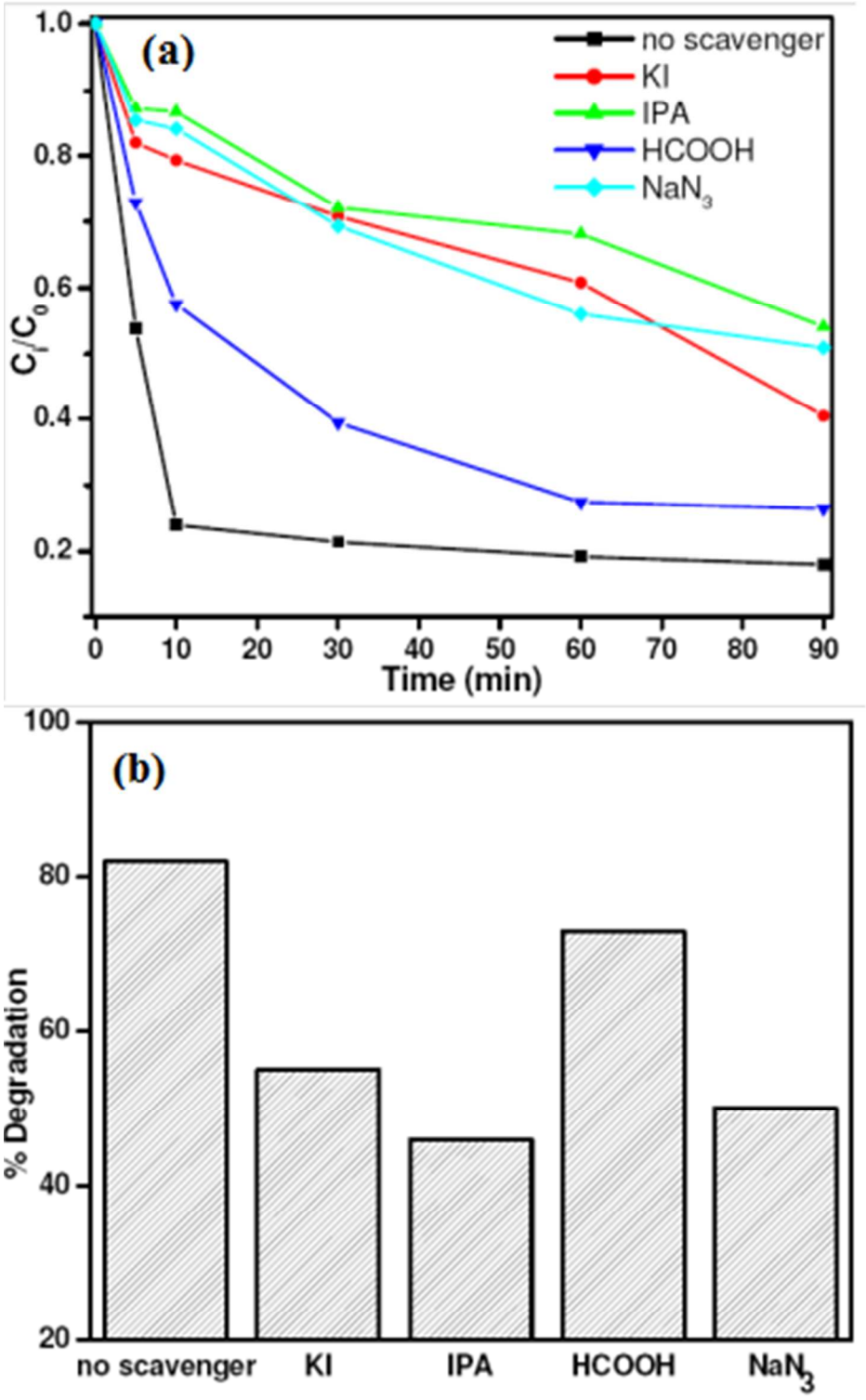

Figure-12

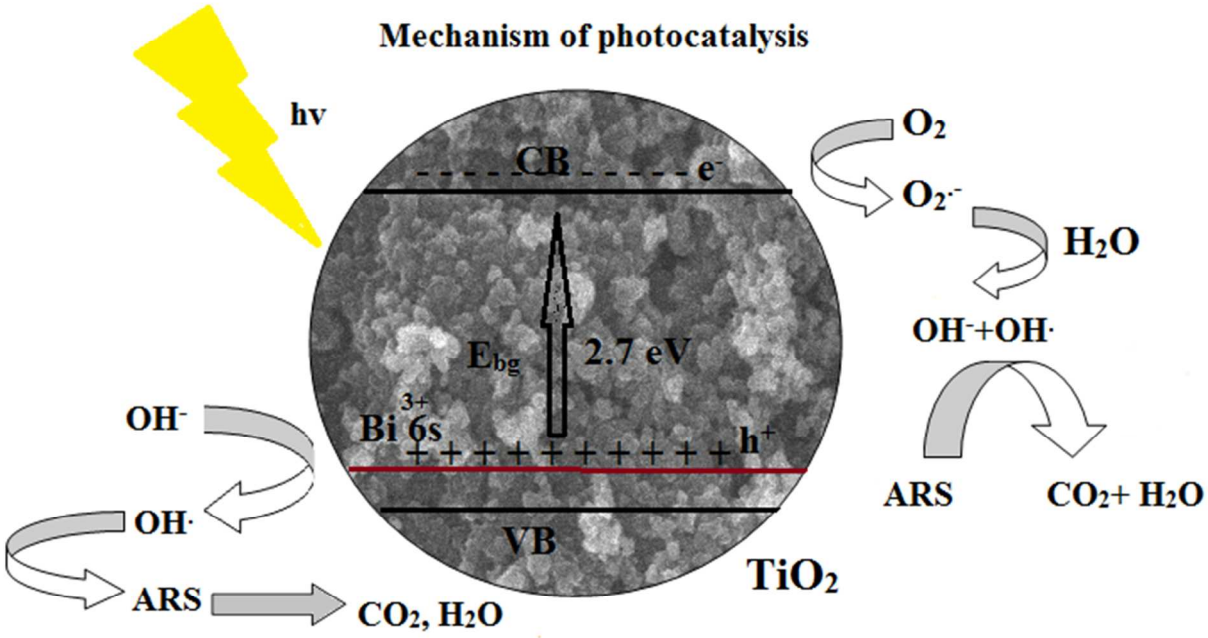

Figure-13

Table captions

Table1. Surface area, pore volume and pore radius obtained from different methods for 1% BiT catalyst.

Table 1

Method	Surface area (m^2/g)	Pore volume (cc/g)	Pore radius Dv(r) nm
BJH	122.14	0.263	4.353
DH	124.34	0.258	4.353
DFT	101.64	0.258	3.112

Table2. Comparison ofsurface area obtained fromthemultipoint BET method (adsorption data in the P/P_0 range 0.05–0.3 for TiO_2 P25 (Degussa), synthesized TiO_2 and 1% BiT catalysts.

Table 2

S.No.	Catalyst	BET Surface area (m^2/g)
1.	1% BiT	126.16
2.	P25 TiO_2	58.2
3.	Prepared TiO_2	95.42